Published in final edited form as:
J Chem Ecol. 2008 July ; 34(7): 837–853. doi:10.1007/s10886-008-9490-7.

Physical Processes and Real-Time Chemical Measurement of the Insect Olfactory Environment

Jeffrey A. Riffell[1,3], **Leif Abrell**[2,3], and **John G. Hildebrand**[1,3]
Jeffrey A. Riffell: jeffr@neurobio.arizona.edu; Leif Abrell: ; John G. Hildebrand:
[1] ARL Division of Neurobiology, University of Arizona, Tucson, AZ 857210-0077, USA
[2] Department of Chemistry, University of Arizona, Tucson, AZ 85721, USA
[3] Center for Insect Science, University of Arizona, Tucson, AZ 85721, USA

Abstract

Odor-mediated insect navigation in airborne chemical plumes is vital to many ecological interactions, including mate finding, flower nectaring, and host locating (where disease transmission or herbivory may begin). After emission, volatile chemicals become rapidly mixed and diluted through physical processes that create a dynamic olfactory environment. This review examines those physical processes and some of the analytical technologies available to characterize those behavior-inducing chemical signals at temporal scales equivalent to the olfactory processing in insects. In particular, we focus on two areas of research that together may further our understanding of olfactory signal dynamics and its processing and perception by insects. First, measurement of physical atmospheric processes in the field can provide insight into the spatiotemporal dynamics of the odor signal available to insects. Field measurements in turn permit aspects of the physical environment to be simulated in the laboratory, thereby allowing careful investigation into the links between odor signal dynamics and insect behavior. Second, emerging analytical technologies with high recording frequencies and field-friendly inlet systems may offer new opportunities to characterize natural odors at spatiotemporal scales relevant to insect perception and behavior. Characterization of the chemical signal environment allows the determination of when and where olfactory-mediated behaviors may control ecological interactions. Finally, we argue that coupling of these two research areas will foster increased understanding of the physicochemical environment and enable researchers to determine how olfactory environments shape insect behaviors and sensory systems.

Keywords

Odor plume; Insect behavior; Odor-plume tracking; PTRMS; Mass spectrometry; Gas chromatography; Odor landscape

Introduction

Since animals crawled onto land approximately 400 mya, they have had to contend in a terrestrial, chemosensory environment where airborne signals are chemically different and fluctuate faster than under water. Airborne chemicals must have coevolved with multicellular organisms, especially with the large Angiosperm and insect diversification about 100 mya (Hildebrand 1995; Zimmer and Butman 2000; Bargmann 2006). In water or in air, the

Correspondence to: Jeffrey A. Riffell, jeffr@neurobio.arizona.edu.
Notation for Physical Processes and Analytical Technologies, respectively, is summarized in Appendices 1 and 2.

extraction of necessary chemical information from the environment has always depended upon discriminating signal from noise and resolving distance and orientation to the source.

In the last 25 years, efforts aimed at understanding how chemical signals are distributed in space and time have gained traction in a research discipline traditionally focused on identifying the behaviorally important chemical signals. A realization has occurred that the physical environment determines (a) whether or not and how much chemical signal is available to the animal and (b) the behavioral response and navigational strategies used by the recipient organism (Weissburg and Zimmer-Faust 1993; Mafra-Neto and Carde 1994; Vickers and Baker 1994). A number of studies, pioneered by Murlis and Jones (1981), have documented that chemical signals are dynamic in both space and time (Murlis et al. 2000a; Justus et al. 2002b) due to physical processes of the fluid environment (Murlis and Jones 1981; Elkinton et al. 1984; Moore and Atema 1991; Murlis et al. 2000b; Webster and Weissburg 2001; Justus et al. 2002b). Seminal work by Baker and Cardé, in turn, has demonstrated that the physical environment dictates the navigational behavior employed by an organism through its effects on controlling the information provided by the chemical signal (Willis and Baker 1988; Mafra-Neto and Carde 1994; Vickers and Baker 1994; Kuenen and Carde 1994; Willis et al. 1994; Zimmer-Faust et al. 1995; Vickers and Baker 1996). The aerodynamic environment can dictate important ecological interactions and be a selective force on the evolution of olfactory systems, as it determines the chemical information available to an organism (Hildebrand 1995; Zimmer and Butman 2000).

The olfactory systems of terrestrial animals sample the environment and process chemical stimuli faster than once per second, but most chemical analysis methods for behaviorally relevant volatiles require extended time periods for sample collection, preparation, and separation (Tholl and Röse 2006). Thus, the temporal resolution of the olfactory information traditionally has been lost to scientists. New analytical technologies involving fast (<1 s or <1 min) sampling times and quantitative resolution are becoming available for chemical ecologists, thereby providing a means to sample the odor environment at time scales approaching that of the insect olfactory system.

In this review, we examine how the physical environment constrains olfactory-guided behavior by considering five main ideas. First, because the fluid environment controls the chemical information available to an organism, a review of some simple, but critical, physical processes that can provide linkages between the physical environment and odor-mediated behavior are considered. This information hopefully will provide researchers a set of tools to aid in characterizing the physical environment. Second, a qualitative description of the different characteristics of a turbulent odor plume is reviewed. Third, we consider the different physicochemical environments that insects navigate in. Fourth, we examine the effects of body size on the odor landscape experienced by a navigating insect. Whether an animal is <1 mm or >10 cm will potentially influence the physicochemical landscape in which it exists and the sensory strategies that it utilizes. Last, we examine the current analytical technologies available to chemical ecologists and behavioralists to examine spatial and temporal distribution of chemicals that control behavior. Taken together, the aim of these sections is to provide a broad understanding of the physical factors that control odor information and behavior and the rapidly evolving technologies that may increase our understanding of these processes.

Physics of the Odor Environment

Once odorant molecules evaporate from a source, they will instantly become subject to the physical forces of the environment and transported by ambient motions of the air. There are two physical processes that influence the transport of odor at different spatial scales: molecular diffusion and turbulence and advection. Molecular diffusion transports odorants by Brownian

motion and occurs under small spatial scales (<1 mm) and long time periods (ca. 80 min for an odorant molecule to travel 1 m). In contrast, ambient motion by air can transport odorant molecules >10^3 times quicker than diffusion over equivalent distances and is thus the principal physical process that controls odor transport at distances >1 cm.

At these much larger spatial scales, the odor environment is dynamic, both spatially and temporally. There are two physical processes that cause this variability: advective and turbulent transport. Advection is the bulk transport of the odorants by the mean direction of the flow, whereas turbulent transport comprises the chaotic, three-dimensional mixing of odor with clean air. By using Gaussian distribution models for pollutant transport, researchers initially modeled chemical plumes as a diffusive, time-averaged process. However, the sensory systems of animals flying or walking in the terrestrial environment rarely, if at all, use such time-averaged odor information. Instead, animals use near-instantaneous concentrations of the odor plume to navigate to a source. It is, therefore, important to understand the near-instantaneous resolution of odor information to determine how animals can locate odor sources. To understand this process, it is necessary first to understand the physical forces that control odor information at these spatial and temporal scales. Excellent reviews of the instantaneous structure of plumes are found in Murlis et al. (1992), Weissburg (2000), and Koehl (2006). In this review, we examine physical processes and parameters useful to characterize the odor dynamical processes and the rapidly evolving analytical technology that may be used to characterize the terrestrial chemical environment.

Aerodynamic Parameters

Odor temporal dynamics and dispersion are governed by ambient air currents. An insect living in a calm, low wind environment will experience different chemical stimulus dynamics from one inhabiting a high-energy, windy environment. A measure of the fluid dynamic regime experienced by a navigating insect can be approximated by the body Reynolds number (*Re*), which compares the inertial forces with viscous forces. Inertial forces represent the large momentum-containing scales that maintain the turbulent motion. In contrast, the viscous forces signify the “stickiness” of the fluid that dampens the momentum, thereby bringing it to a halt. The inertial term takes the form of ρu^2 [where ρ is the density of air (kg/m^3), and u is the wind velocity or translational velocity of the organism (m/s)], and the viscous term takes the form of $\mu u/S$ [where μ is the air viscosity (Ns/m^2), and S is the spatial scale of interest (m)]. The ratio of these two forces thus takes shape in the equation as

$$Re = \frac{\rho u^2}{\mu u/S} = \frac{\rho S u}{\mu}, \quad (1)$$

thereby producing a non-dimensional number that indicates the nature of the air flow. When $Re \gg 1$, the air momentum will overwhelm viscous damping, and air motion will be turbulent. As *Re* increases, the air flow becomes more turbulent and causes the spatial scale of the turbulence to increase (e.g., the size of the turbulent eddies) and the time scales of the turbulent fluctuations to increase. As *Re* decreases and approaches unity, the spatiotemporal dynamics of the turbulent flow decrease until the flow becomes laminar (without three-dimensional structure).

The Reynolds number is useful for examining the fluid environment an organism might experience, but to accurately replicate the aerodynamic conditions of the field within the laboratory, it is necessary to go beyond the mean advective bulk flow and instead examine the fluctuations (turbulence) of air flow. Fluid (liquid or gas) near any surface will stick to the surface and not slide along that substrate. Due to this “no-slip” condition, the fluid in contact

with the substrate will impose a frictional force on the fluid layers directly above it causing the fluid to shear or change in velocity with increasing distance from the substrate (Fig. 1A). Within this velocity gradient region—also called the "log layer" because of the logarithmic change in velocity with vertical distance from the substrate—momentum is transferred from the large turbulent structures (called 'eddies') to progressively smaller and smaller eddies until energy is dissipated into heat by the frictional force of viscosity near the surface (Fig. 1A). Thus, turbulence can be much greater near the surface than in the region of the free-stream velocity. The turbulence and momentum transfer to the surface can be described through shear stress (τ_R) (also called Reynolds shear stress) and is a the function of

$$\tau_R = -\rho\overline{u'w'}, \tag{2}$$

where the term $\overline{u'w'}$ is the mean of the cross–product of fluctuating velocities in the horizontal (u) and vertical (w) dimensions, and the negative term in front of the air density (ρ) denotes the downward flux of momentum. The Reynolds shear stress provides a measure of the turbulence of a system. Another term for describing boundary layer turbulence is the friction velocity (m/s), u_*, and is related to the shear stress by $(\tau_R/\rho)^{-1/2}$. This term has the units of a velocity (m/s) but is more accurately described as the scalar of momentum in a boundary layer or the velocity at which momentum is transferred. As u_* increases, turbulent fluctuations in velocity also increase; therefore, u_* is an important scaling parameter in boundary layer and turbulent wind studies. The turbulent conditions of a boundary layer (e.g., a large grassy meadow or a desert plain) can be parameterized through the roughness Reynolds number (Re_*), which is analogous to the Reynolds number described above but provides a means to describe the turbulent conditions of a boundary layer. This term is described by the equation

$$Re_* = \frac{\rho u_* D}{\mu}, \tag{3}$$

where D is the size (m) of the elements on the substrate (e.g., the rocks and vegetation on the ground), and u_* is the friction velocity described above. For Re_* values of 3.5–6, turbulent eddies begin to penetrate the upper region of the boundary layer, and if $Re_*>75$, then turbulence extends all the way to the substratum (Schlichting 1987; Stull 1988). An insect navigating to an odor source within a boundary layer of $Re_* >75$ will experience a dynamic, filamentous odor stimulus, whereas an insect navigating at $Re_*<6$ will experience a smooth continuous odor gradient near the substratum (where diffusional and inertial processes are near unity) and a filamentous odor stimulus farther from the substratum.

The roughness Reynolds number provides a useful parameter to describe certain environments (further detailed below), but caution must be used as it may not accurately describe the dominant physical processes for a given habitat. For instance, the velocity fluctuations of a meadow sat the foot of a 1,000-m-tall mountain will reflect the influence of the mountain on the atmospheric conditions rather than the grass and shrubs found within the meadow (D=1 m), thereby causing underestimation between realized and expected Reynolds roughness numbers. Therefore, the length scale, D, used in calculating Re_* should be chosen carefully. Nevertheless, measurement of τ_R and u_* provides valuable information regarding the level of turbulence in a given habitat and also allows these physical conditions to be simulated in the laboratory for dynamically scaled odor-plume tracking studies (Zimmer and Zimmer 2008).

In the field, an important function of the stability, or lack thereof, of the boundary layer is the atmospheric conditions (temperature and air turbulence). In the absence of energetic

atmospheric events that mix the atmosphere, like frontal passages, daytime temperature-induced convection occurs from heating of the surface, causing large eddies to form and thoroughly mix the air from the surface to >1 km height (Figs. 1B and 2A,B; Kaimal and Finnigan 1994;Mole and Jones 1994). In contrast, at sunset, the temperature-driven convection weakens, and a stable boundary layer develops near the surface (0–200 m; Fig. 1C and 2A,B;Mylne 1992;Yee et al. 1993;Mole and Jones 1994). The stability of the boundary layer can be determined through the Richardson number (R_i), which is a dimensionless parameter that represents the relative importance between temperature- and wind-driven turbulence and has the form

$$R_i = \frac{(g/\bar{\theta})(\partial\bar{\theta}/\partial z)}{(\partial\bar{u}/\partial z)^2}, \quad (4)$$

where g is the acceleration due to gravity (9.81 m/s^2), $\bar{\theta}$ is the mean temperatures, z is the height above the substrate, and $\bar{u}$ denotes the mean wind. When R_i is positive, the boundary layer is stable (Fig. 1C). R_i is negative for an unstable boundary layer (Fig. 1B) and zero for a neutral boundary layer. For example, Mole and Jones (1994) found that plume intermittency, filament concentration, and average concentration were higher for stable than for unstable conditions. Thus, when atmospheric conditions are relatively calm and uncloudy, the odor environment at night might be conducive for odor plume transport and the maintenance of plume structure and hence insect navigation (e.g., Fig. 2C).

The Odor Landscape and Turbulent Odor Plumes

Examination of olfactory tracking behavior of insects, mammals, and birds (all inhabitants of turbulent flows) has demonstrated clearly that animals do not use time-averaged properties of the odor (Elkinton et al. 1984) and instead use near-instantaneous (< 1 s) information present in the plume (Mafra-Neto and Carde 1994; Vickers and Baker 1994).

Temporal Features of the Plume—At time and spatial scales <1 s and >1 mm, respectively, turbulent odor plumes are patchy (Fig. 3B) and are composed of odor spikes or ‘filaments’ of intense concentration interspersed with periods and regions of low or undetectable concentrations. The dynamic occurrence of the chemical signal is termed its intermittency, which is a proportional value ranging from 0 (odor continuously present) to 1 (odor absent; Cardé and Willis 2008). The spatial and temporal scales in which the odor filaments occur are directly related to the temporal and spatial scales of the turbulence (Fig. 3B;Zimmer-Faust et al. 1988).

A number of different factors can influence plume intermittency. A higher wind speed or turbulence can cause the odor filaments to become thin (Yee et al. 1993) and increase in frequency (more filaments per unit time; Fackrell and Robins 1982). However, an increase in turbulence has a corresponding effect of lowering the odor-laden filament concentration (Finelli et al. 2000; Moore and Crimaldi 2004). Moreover, the size and position above the substrate of an odor source also affects the plume dynamics. Odor sources high off the substratum will be subject to higher advective flows than those nearer the ground (Fig. 1C). For instance, flowers of the agave, *Agave palmeri*, which produce strong night time odor emissions, are 4–6 m from the ground and are subject to high advective wind velocities (2.2–7.1 m/s). Whereas flowers from the jimsonweed plant, *Datura wrightii*, are close to the ground (~0.5 m) and experience lower wind velocities (0.1–2.3 m/s). Odor source size will also affect the plume structure close to the source. For example, plume intermittency is higher for larger sources than smaller, but if a small source is in close proximity to a large structure (e.g., a

female moth calling from a tree), then the plume will behave as if coming from the large structure. A rough approximation of the effects on odor source size and air velocity on plume intermittency may be determined by the Strouhal number (*St*), which relates to the frequency in which eddies are shed by structures in flow. For cylindrical objects, the eddies are shed with a predictable rate,

$$St = \frac{f D_{\text{object}}}{u}, \tag{5}$$

where f is the frequency of eddy shedding (per second), and D_{object} is the diameter of the object (m). Eddies shed by the object will entrain the odor and impose a dominant frequency on the olfactory information transmitted in the object's wake. For smooth cylinders in the Re range of 10^2–10^5, *St* is a constant of 0.2, thereby allowing rearrangement of the equation for the dominant eddy frequency (and hence, plume intermittency) to be $f=0.2u/D_{\text{object}}$. We caution use of *St* in the field, however, under conditions of strong, three-dimensional winds, which will change the projected diameter of the obstacles (D_{objects}) thereby affecting the plume filament frequencies. Another aspect that can influence the temporal features of the odor plume is "active" behavior by the animal (or source) releasing the odor. For instance, female moths can periodically pump pheromone into the air (Conner et al. 1980) and flowers in the wind oscillate back and forth (Sprayberry and Daniel 2007). The intermittent release and odor source movement will influence the temporal structure of the plume signal, thereby creating a biologically mediated intermittency coupled to that of the turbulent flow.

Spatial Structure of the Plume—The plume structure will change as a function of the distance from the odor source (Fig. 3). Research by atmospheric scientists who study pollutant transport for the past 30 years have scoured the countryside searching for large (~1 km), flat (~10 cm vegetation height) sites in which to examine the effects of boundary layer turbulence on plume structure. Experiments on the fields in UK, Canada, and USA provide a framework for understanding the effects of turbulence on odor plume structure (Mylne and Mason 1991;Yee et al. 1993;Mole and Jones 1994). For plumes on a relatively flat surface, the plume increases in width and height and decreases in filament intensity and intermittency (the proportion of time odor is present) as distance from the source increases. For instance, Dinar et al. (1988) found that chemical signal concentration in a plume was high and present 75% of the time at a position <4 m downwind from the source, but concentrations dropped to 20% and occurred only 20% of the time at 40 m downwind (Dinar et al. 1988). Similarly, Murlis (1997) found that the chemical signal in a plume was present 40% of the time at a position 2.5 m downwind from the source but only present 10% of the time at 20 m downwind (Murlis 1997).

A conceptual model of the effects of turbulence on the large-scale plume structure can be based on the size of the turbulent eddies mixing the plume. For instance, Mylne (1992) described the formation of a plume based on its width relative to eddy size present in the turbulent flow. When the plume width is narrower than the dominant eddies, then the plume will meander (move side-to-side), thereby creating large patches of odor-laden air interspersed with odor-free air (Fig. 3A; Yee et al. 1993; Mylne et al. 1996; Finelli et al. 1999). As the plume width approaches or exceeds the dominant eddy length scale, vigorous mixing occurs with non-odor laden air transported into the interior of the plume (Fig. 3A). The distance that plumes meander can be estimated by u/n, where n is the frequency of the peak intensity of the velocity power spectrum (e.g., the dominant energy-containing eddies) and u is the wind velocity (Yee et al. 1993). Taking the range of velocities (0.2–2.0 m/s) and eddy frequencies (0.01–1.0/s) from Yee et al. (1993), Mylne and Mason (1991), and Murlis (1997), eddy lengths responsible for

plume meandering range from 0.2 to >200 m. While this analysis may only approximate plume meandering under stable atmospheric conditions, it demonstrates the extreme odor patchiness that an insect must navigate toward.

While plume meandering will be critical for the large-scale structure of the plume, the edges and interior of the plume are dynamic and consist of fine-scale features important for navigating animals. For instance, the concentration of chemical signals in filamentous plumes is lower farther from the source in the along-wind direction; although some odor filaments of high concentration do occur, they are encountered much less frequently (Murlis et al. 1992Murlis et al. 2000a; Murlis 1997). The intensity of concentration fluctuations also decreases with distance from the source (Murlis et al. 1992; Zollner et al. 2004). Moreover, with increasing distance from the center of the filamentous plume to the edges in the crosswind direction, odor intensity and intermittency also decrease (Mylne and Mason 1991; Yee et al. 1993; Murlis 1997). Although odor filaments occur less frequently on the edges of the plume than near the centerline, the concentration of the filaments can be as high as those in the middle.

The Dynamics of a Plume in a Laboratory Wind Tunnel—Until now, we have focused on the dynamics of an odor plume in fairly idealized conditions: large area (~1 km), short vegetation (~10 cm), and steady turbulent wind conditions. Under these conditions, the plume will grow and meander. Can all of these conditions be replicated in the laboratory wind tunnel? Unfortunately, the size of a typical wind tunnel (~0.5–1 m^2 height and width and 2–5 m length; Visser 1976; Miller and Roelofs 1978) is much smaller than the dominant turbulent length scales in the field (1–200 m); therefore, a plume in a wind tunnel will not exhibit the same characteristics. However, physical turbulent conditions in the field, including turbulent fluctuations (root-mean-square velocity divided by the mean velocity) and Reynolds stresses, can be simulated in the laboratory to approximate those forces in the field (Cermak and Arya 1970; Fackrell and Robins 1982; Justus et al. 2002). Such scaling parameters are paramount, as they are necessary to replicate a natural aerodynamic regime and will dictate the plume spatiotemporal characteristics. Turbulent conditions in the field involve both the advective (mean velocity and direction) and turbulent (fluctuating velocities) components of the wind, as well as a number of other parameters that involve wind gusting (acceleration reaction) and change in direction. However, researchers that use wind tunnels have tended to simulate complex wind conditions by using single velocity measurements or, at best, single Reynolds numbers. Before beginning a behaviorally oriented, odor plume study, it is essential to determine the number and nature of the critical wind parameters (Fig. 2). Otherwise, reproducibility (i.e., dynamic similarity) is difficult to achieve (Zimmer and Zimmer 2008).

Environmental Effects on the Odor Landscape

Turbulent motion and molecular diffusion will spread a chemical plume in three dimensions to create what may be viewed as an odor landscape (Atema 1996; Murlis 1997; Zimmer and Butman 2000) in which an animal must navigate. The degree to which these motions dominate odor transport depend largely upon the physical environment. For habitats that are relatively flat (e.g., a large, grassy meadow, or a sandy plain), a useful rule of thumb for establishing the turbulence of the physical environment is by the roughness Reynolds number (Re_*). Re_* depends upon the shear velocity (u_*) and the roughness element (D) (Schlichting 1987). Therefore, the three-dimensional environment where odors are released will determine the odor intensity and spatiotemporal dynamics.

Odor Dynamics on a Desert Plain

A large, sandy plain, for example, near Maharès, Tunisia, provides an excellent example for effects of the roughness element on boundary layer turbulence. The degree to which turbulent eddies from the atmosphere come into contact with the substrate depends in large part on the

size of the roughness element and wind velocity. For a shear velocity of 0.4 m/s (Wolf and Wehner 2000) and average sand grain size of 0.00025 m, the Reynolds roughness number is 6.5. At this number, turbulence begins to reach the outer regions of the boundary layer (Schlichting 1987), and the odor plume will be dominated by advection rather than large turbulent eddies thereby causing the odor plume to become a sheared continuous gradient (Weissburg 2000; Wolf and Wehner 2000). In contrast, if the sand size increases to 0.0025 m and the u_* remains 0.4 m/s, the Re_* is 65.8, which indicates that turbulent eddies are close to reaching all the way to the substrate, and hence, the boundary layer (and the odor plume) is fully turbulent. This raises an important point: The presence of roughness on the substratum decreases the velocity, which causes the boundary to become fully turbulent, and hence turbulence changes as a function of roughness element size. Observations of smoke used to simulate a plume for odor-tracking ants in this desert environment suggests that the Re_* values may be ca. 6, with the smoke remaining close to the substrate and becoming “smeared” by the low wind velocity.

Odor Dynamics in a Field

In more heterogeneous habitats, substrate differences and wind velocity begin to play a larger role in controlling the odor. For instance, by using the same shear velocity from the example above in the desert (0.4 m/s; Yee et al. 1993; Mole and Jones 1994) but using vegetation height as our roughness element (0.1–1.0 m), we find that the roughness Reynolds number ranges from 2,630 to 26,300. Because turbulence will fully dominate this habitat under a variety of spatial and temporal conditions, the odor landscape will also be dynamic reflecting the three-dimensional fluctuations in velocity. For instance, Yee et al. (1993) found that because of the large eddy sizes associated with the field environment (u_*=0.25–7.0 m/s; D=0.5 m; Re_*=3,290–13,200), plume meandering only occurred close to the plume source, and at larger downwind distances (>100 m), the plume became well mixed, lacking a large-scale meandering structure but still being highly intermittent (Yee et al. 1993). Hence, a foraging insect far from a food odor source may experience a wide plume that has fine-scale structure and odor intermittency, but as it approaches the source—due to plume meandering and the plume width decreasing—the odor signal will become more spatiotemporally complex with longer periods of odorless air.

Odor Dynamics within a Forest

In contrast to the relatively flat surfaces of a grassy field or desert plain, the physical environment within a forest is dynamic and depends upon the vertical location between the canopy and the floor. Whereas Re_* provides a good rule of thumb for boundary layer turbulence in field and desert environments, forest habitats are so spatially complex that a developed boundary layer does not exist. This is because the upper canopy and large diameter tree trunks constrain large eddies from entering the understory regions of the forest, and thus, turbulence, radiation, thermal, physiological, and structural properties of a forest vary most in the vertical dimension (Rauner 1976; Hutchison and Baldocchi 1989), where turbulence levels are maximal near the upper canopy and decline rapidly in the understory toward the shrub layer and forest floor (Baldocchi 1989). Thus, in the understory, turbulence levels are low (u_*=0–0.2 m/s), the length of the turbulent eddies are small (1–3 m), and the bulk advective motion of the wind is minimized (0.1–1.0 m/s) relative to the turbulent eddies which cause the wind direction to shift chaotically (Kaimal and Finnigan 1994).

Studies that examine the transport of the tracer sulfur hexafluoride (SF_6) within a forest have shown that plume concentrations exhibit a logarithmic decrease in concentration with increasing distance from the source. For example, LeClerc et al. (2003) and Thistle et al. (2004) showed that mean tracer concentrations drop from 20% within 5 m of the source to 0.1% 60 m downwind. Moreover, individual filament concentrations can be tenfold higher than

the average concentrations 10 m from the source, with the plume being intermittent and time between odor bursts long (40–300 s) in duration. An interesting phenomenon that affects plumes is the lack of a strong advective wind velocity, which causes the odor plume to swing back and forth extending in two directions 180° opposed (Leclerc et al. 2003; Thistle et al. 2004). Thus, a flying insect moving from a meadow into the forest will experience a totally different physical environment that may require different sensory strategies for navigation.

Effects of Scale

An important aspect that influences the odor environment experienced by animals is body size and translational speed —or wind velocity—of the animal itself. Returning to the Reynolds number, which indicates the ratio of inertial to viscous forces, and is the product of the size and speed, we can begin to examine the odor landscape experienced by insects of different sizes.

Small insects will experience a completely different physicochemical environment from larger, faster insects. The leaf-cutter ant, *Atta vollenweideri*, provides an interesting example of the effects of small size and the environment for the type of forces experienced by the ant. For instance, leaf-cutter ants are small (ca. 0.005 m) and, when in their nest, experience air flows of 0.005–0.02 m/s (Kleineidam and Roces 2000; Kleineidam et al. 2001) with corresponding Reynolds numbers of 1.6–6.5. Within this environment, ants experience a fluid dynamic regime where viscous forces nearly balance inertial forces. This will have an important effect on the odor landscape by smoothing out three-dimensional structures of the flow and hence causing the odor plumes to become sheared gradients. In contrast, when these ants leave their nest, they experience a grassy field environment with wind velocities of 1–6 m/s and the corresponding $Re>300$. In this environment, the odor will be fully turbulent and dynamic. For much larger or faster insects ($S\geq0.02$ m, $u\geq0.5$ m/s), for example, the flying hawkmoth *Manduca sexta*, Reynolds numbers are typically 1,000–10,000. These insects, then, exist in a fully turbulent environment where the odor will be intermittent and three dimensional.

Analytical Equipment

Role of Technology

In the previous sections, we detailed how atmospheric and landscape conditions may distribute chemical odors spatiotemporally. Valid measurements of something as amorphous as an odor plume may seem currently inaccessible. Nonetheless, to be able to measure chemical signals in real time as they are emitted and perceived by the organism is critical for determining how chemical signaling processes determine ecological and evolutionary interactions. Therefore, a continuous goal is the acquisition of improved technologies that will provide rapid and sensitive chemical data, which can then be merged with behavioral or electrophysiological observations and integrated into a mechanistic description of olfactory ecology.

A grand challenge to improve the sensitivity of our analytical measurements was unintentionally laid before us nearly 40 years ago when Kaissling and Priesner (1970) discovered that, by using olfactory receptor cells on sensilla structures lining their antennae, male moths can detect a single pheromone molecule. Although fluorescence detection and other techniques have pushed limits of chemical detection into the zeptomole (10^{-21}) range, today, we still appreciate the animal nose (or insect antenna) as a type of ultimate detector.

Animal olfactory receptors remain supreme not only for their molecular sensitivity but also for their respectable sample collection speed. *M. sexta* moths, a favorite model organism, optimally collect odor samples in the range of one to five times per second (1–5 Hz; Heinbockel et al. 1999), but *Spodoptera exigua* and *Cadra cautella* moths have been shown to exhibit

electroantennographic responses to stimulus intermittencies given at up to 33 Hz (Bau et al. 2002). Modern analytical techniques can also collect samples at this rate, and faster, but in most cases, these instruments are tuned to a single chemical identity. For the best information about chemical identification, gas chromatography mass spectrometry (GCMS) has remained the most reliable and popular technique for many years, but sample collection for this method is traditionally slow. Recently, GCMS sensitivity has become quite high (10^{-12} g; Song et al. 2006). Analytical equipment available to chemical and olfactory ecologists will be reviewed in the context of analyzing odor dynamics with maximal sensitivity, speed, and accurate chemical identification, where unfortunately one feature is often sacrificed for improvement of the others. Examples will range from commercially available devices to emerging technologies that tend to appear first as applications in atmospheric chemistry or in monitoring industrial environments.

Valuable reviews have addressed aspects of modern instrumentation and sampling methods useful for temporally analyzing biogenic volatile organic chemicals (BVOCs). Tholl et al. (2006) specifically address challenges and advances in monitoring environmentally dependent changes in plant volatile emissions by including in-depth descriptions of instruments, sampling techniques, and respective biases and limitations. D'Alessandro and Turlings (2006) pay special attention to above- and below-ground sampling techniques for herbivore-induced plant volatiles that mediate interactions among plants and insects. Ten emerging sensor technologies from the US Sandia National Laboratories for volatile organics monitoring are reviewed by Ho et al. (2007), and a recent review on electronic noses by Röck et al. (2008) discusses the integration of multiple sensor techniques. In this review, we focus on chemical detection technologies (and other supportive techniques) that feature low limits of detection, and rapid temporal measurement capability as a strength for maximum resolution of odor dynamics, and portability is emphasized.

Gas Chromatography

Terrestrial animal olfactory systems sample the environment and process chemical stimuli faster than once per second. In contrast, popular methodologies for analysis of behaviorally relevant volatiles involve significant time periods for collection, preparation (e.g., concentration or cryofocusing), and separation. The introduction of these samples into analytical instruments for structural characterization and quantification (e.g., by GCMS) usually results in significant loss of temporal resolution of the chemical signal. However, new, fast (ca. 200–400 s run times) GC systems are becoming available for chemical ecologists, thereby providing a means to sample the odor environment at time scales more relevant to moving, probing insects. Matisola and Dömötörová (2003) review multiple design strategies employable for streamlining GC analysis and provide tabulated examples of different approaches, including a shortlist of field-portable GC systems in use. Many of the these strategies were advanced in the laboratory of the late Richard Sacks, including at-column heating to enhance selectivity, use of atmospheric air as a carrier gas to facilitate portable GC, development of pre-concentrator systems, microelectro-mechanical system silicon columns (etched into a ca. 10 cm^2 chip), and alternative inlet devices and detectors needed to support miniaturization (Reidy et al. 2007; Sanchez and Sacks 2007).

Kunert et al. (2002) demonstrated rapid GC for improved temporal characterization of plant volatile emissions by employing the zNose™ miniature GC with a surface acoustic wave quartz microbalance detector (SAW; Electronic Sensor Technology, Newbury Park, CA, USA; or see Lu and Zellers 2002). They achieved a 3-min time resolution of lima bean volatile terpenoids in response to leaf wounding. By using standard charcoal pre-concentration, this rapid analysis is a drastic temporal improvement over classic GC runs that last 10–60 min. Even without the capability to define odor fluctuations that occur from second to second, this portable technology

is useful in olfactory dynamics for making confident chemical identifications in the field just minutes after sample collection or for creating a temporal odor profile with ca. 3 min temporal resolution (e.g., if left to run continuously and automatically). Other fast GC systems with automated pre-concentration have been custom built for atmospheric monitoring from aircraft and employ helium ionization detection (HID) and electron capture detection (ECD) for selective detection down to parts per trillion level of non-methane hydrocarbons (C_2–C_5) every 5 min (Whalley et al. 2004).

Mass Spectrometry

Chemical Ionization Techniques—Atmospheric pressure chemical ionization (APCI; soft ionization) mass spectrometry techniques for environmental air analysis have attracted much interest (Charles et al. 2001). APCI mass spectrometers performing proton transfer reaction mass spectrometry (PTRMS) and selected ion flow tube mass spectrometry (SIFTMS) are both commercially available. PTRMS has been applied numerous times for measuring BVOCs (De Gouw and Warneke 2007) and has been adapted for measuring BVOC fluxes by using eddy covariance approaches (Karl et al. 2000).

PTRMS uses H_3O as a reagent gas, so that H_3O primary ions travel into a drift tube and collide with gaseous organic volatiles (*M*) by the proton transfer reaction

$$H_3O^+ + M \rightarrow MH^+ + H_2O$$

if energetically allowed (if *M* has a proton affinity exceeding that of water, 166.5 kcal/mol, a condition fulfilled for essentially all VOCs). Quadrupole unit mass detection limits of 5–30 ppt have been reached, and measurement times can be as low as 2 ms per observed ion, thus allowing real-time monitoring of ambient air in environmental situations that include aircraft flight missions and extended environmental sampling campaigns (Lindinger et al. 1998a, b). At 130 kg, the PTRMS is portable on wheels or can be lifted by several people for short distances. PTRMS is also available with high resolution time of flight (HRTOF) mass detection and has been adapted with a GC inlet and ion trap (IT) detection. SIFTMS also employs a quadrupole for detection limits of a few parts per billion and measurement times of a few seconds (Freeman and McEwan 2002). An additional upstream quadrupole filter is used to select reagent gas ions of H_3O^+, O_2^+, NO^+, or others. The instrument is similar in size and cost with quadrupole PTRMS. APCI inlets on benchtop liquid chromatography (LC)ITMS instruments have also been successfully modified to accept gas samples with rapid measurement times of 20–200 ms per observed ion (Jublot et al. 2005).

PTRMS has been used in a variety of different applications that involve emission of volatile compounds. Karl and others have used PTRMS for examining dynamics of green leaf volatiles, pollutants, and herbivory-induced changes in volatile emissions from plants (Karl et al. 2003; von Dahl et al. 2006; Filella et al. 2006). Recently, we have used PTRMS to measure synthetic floral odor plumes simultaneously with insect electroantennography measurements in wind tunnels. Raw and processed data both appear as a temporal evolution of mass intensities for a single, or multiple ions, over a particular time period (PTRMS measurement of a single odor species for a 190 s time period is shown in Fig. 3B).

Sample Desorption Techniques—A desire to analyze samples under ambient conditions (outside of the vacuum area) has driven the development of ambient desorption techniques. Desorption ionization (DI) techniques can use a laser or charged particles (i.e., an electrospray) to dislodge and ionize ambient sample particles for introduction into a mass spectrometer (Cooks et al. 2006). The popular desorption electro-spray ionization (DESI) method works

well typically on solid samples. Numerous related techniques have evolved, some of which accommodate gaseous samples, like the direct analysis in real time (DART) method, which uses an excited gas (plasma) to drive the desorption process of solid, liquid, or gas samples (Cody et al. 2005; Haefliger and Jeckelmann 2007), or atmospheric pressure Penning ionization (APPeI; Iwana et al. 2006), which uses argon or helium (rare gases) activated by a negative-mode corona discharge to ionize a pulled gaseous sample before analysis by TOFMS. Laser photoionization of trace gas molecules has been developed mainly along two, parallel paths: resonance-enhanced multiphoton ionization time-of-flight mass spectrometry (REMPI-TOFMS) and single photon ionization (SPI) TOFMS (Zimmermann 2005). Real-time gas sample analyses (e.g., coffee roasting emissions at 10 Hz; Dorfner et al. 2004) have been achieved by using REMPI-TOFMS, a selective ionization method for aromatic and highly unsaturated compounds. SPI-TOFMS is a less selective ionization method that allows detection of aliphatics and aromatics. Although the DI techniques above have not yet been directly applied to volatiles from plants or insects, their high temporal resolution, direct gas sampling, and limits of detection present promising opportunities for olfactory ecology (e.g., Fig. 4). Neutral desorption of analytes by extractive electrospray ionization (EESI; Chen et al. 2007) has been used to analyze human breath and also appears to hold promise for applications in ecology.

Alternate Analytical Technologies

Ion Mobility Spectroscopy—IMS is broadly applied today for detecting trace chemical substances, notably in screening air travelers' carry-on baggage for detection of chemical weapons. Eiceman et al. (1990) characterized methylsalicylate ($C_8H_8O_3$) and dimethylsulfoxide (C_2H_6OS) odor plumes in a continuous field setting with IMS in an early environmental application. IMS functions under atmospheric pressure wherein different ion species travel through a buffer gas in a small (ca. 3–15 cm length) chamber (a.k.a. drift tube; also used in PTRMS) along an electric field at different rates, depending on individual mobility, which is determined by mass, charge, and collision cross-section (Borsdorf and Eiceman 2006). IMS techniques based on this concept have evolved for over a century under different names like ion chromatography. The arrival times (i.e., time of flight (TOF); ca. 2–15 ms) of different ion species at the IMS Faraday type detector are used to distinguish them. Short ion travel times allow fast instrument cycling and rapid sampling. Recent advances in IMS have achieved instrument miniaturization and incorporation of new ionization techniques like ESI and corona discharge. More traditional ionization techniques employ CI initiated by radioactive ^{63}Nickel, and photoionization.

Differential mobility spectroscopy (DMS) differs from IMS by the ion path in having two planar electrodes that produce an electric field that oscillates between high and low values (e.g., 500 to 1,500 V) and a sweeping compensation voltage. DMS promises excellent chemical separation for complex volatile organic mixtures in a miniature chip size. Lambertus et al. (2005) detected and separated a complex mixture of 45 organic volatiles ranging from C_2–C_9 at ca. 1–100 ppb by using a 3.0-m GC column on a microchip attached to a 15-mm microchip DMS. High-field asymmetric waveform ion mobility spectrometers (FAIMS) operate similarly to DMS (Borsdorf and Eiceman 2006).

Absorbance Spectroscopies—Volatile organics strongly absorb energy at mid- to far-infrared (IR; ca. 3–1,000 μm) wavelengths, and this makes their detection possible at low concentrations. The near-IR (ca. 0.75–1.4 μm) range is also useful, but detection of VOCs based on overtones in this region is 10^2 less sensitive. Fourier transform infrared spectroscopy (FTIR) is widely used for analysis of many organic compounds, and open-path FTIR (OP-FTIR) is a direct extension of this method for open spaces (from meter to kilometer). Industrial, environmental, and remote sensing applications of OP-FTIR demonstrate its utility. Active

OP-FTIR sensing (includes an instrument light source) is more sensitive than passive sensing (uses ambient light; Vogt 2006). With advanced chemometric techniques, the application of multiple or sweeping OP-FTIR spectrometers and reconstructed tomographic maps has allowed temporal visualization of some vapor plumes (Todd 2000). A direct comparison between OP-FTIR (measurement cycle time 1.2 Hz), PTRMS (ca. 100 Hz), and GC analysis of canister grab samples revealed good agreement with methods that measure parts per billion amounts of volatile organics (Christian et al. 2004).

Several portable laser absorption spectroscopic (LAS) techniques useful for trace gas detection reflect the recent evolution of optical spectroscopy. Small and robust diode lasers with high optical intensity have mostly replaced lamp and filament light sources to provide greater sensitivity and portability for trace gas detections. However, small spectral coverage from these lasers has limited new diode laser dependant devices to the detection of a single gas species per laser. LAS applications in atmospheric science, environmental monitoring, semiconductor production, and breath analysis have demonstrated parts per million–parts per trillion detections of organics of phyto-relevance such as acetone (C_3H_6O), isoprene (C_5H_8), and methanol (CH_4O) among others (Khunemann et al. 2002; Cias et al. 2007; Ngai et al. 2007; Wang and Mbi 2007). Recently, broadly tunable diode lasers have become commercially available in the 1,528–1,608 nm (near-IR) range that are suitable for measuring gases like CO_2 and NH_3, but not appropriate for semiochemical-type VOCs (Kachanov et al. 2006). The lack of availability of lasers in the VOC-appropriate mid-infrared 1,610–1,710 nm range reflects industry needs rather than technological barriers, so commercially available mid-IR laser devices may become more common as the VOC sensor industry matures. Three primary approaches of LAS technology have led to instrumentation that is now available and in use for trace gas detection: cavity ringdown spectroscopy (CRDS), photo acoustic spectroscopy (PAS), and tunable diode laser absorption spectroscopy (TDLAS; Kachanov et al. 2006).

Infrared Gas Analyzer for CO_2 Measurement—Many insects possess olfactory receptor cells that are specifically sensitive to ambient CO_2 levels. Detection of CO_2 concentration changes is important for many insect species (Stange 1996; Guerenstein and Hildebrand 2008). Expression of CO_2 sensory organs among invertebrates appears to be strongest in herbivorous Lepidoptera (Bogner 1990; Stange 1997; Guerenstein et al. 2004). Sexual dimorphism of the CO_2 sensory labial palp organs (LPOs) and sensilla therein is variable among insects. The LI-7500 non-dispersive infrared CO_2/H_2O gas analyzer (LI-COR Biosciences, Lincoln, NE, USA) is the standard tool used by ecophysiologists for measuring precise CO_2 fluctuations from ca. 0–3,000 ppm with response times from 5–20 Hz. The battery operated 0.75 kg instrument is 30×6.5 cm and mountable in any orientation. The LI-7500 has been used to measure dynamic plumes of artificially high CO_2 above host plants inside free air carbon dioxide enrichment (FACE) rings for evaluating the effects of fluctuating, elevated CO_2 on moth oviposition preference (Abrell et al. 2005).

Chemiluminescence—For real-time (10 Hz measurement cycle time) detection (to 400 ppb) of isoprene, Hills and Zimmerman (1990) developed the fluorescent isoprene sensor (FIS) based on detection of chemiluminescence coming from decay of the excited formaldehyde intermediate in the reaction of isoprene (a terminal alkene) with ozone. Other existing chemiluminescence-based trace gas detectors are specific for non-semiochemical type gases.

Insect Antennae as Biosensors—Use of the insect antenna for determination of biologically important volatiles has emerged as an important type of biosensor for specific VOCs, especially pheromones (Roelofs 1984; Park et al. 2002). First, electroantennography (EAG), and later, single-sensillar recording, have emerged as sensitive tools for elucidating behaviorally important volatiles (Schneider 1969; Mustaparta 1975; Guerenstein and Guerin 2001; Stranden et al. 2003). Single-sensillar recording, the electro-physiological recording of

a receptor neuron located on the insect antennae, has been used only in the laboratory due to the delicate arrangement of electrophysiological recording equipment. In contrast, EAGs are robust and have been used in the field. While not as sensitive as single-sensillar responses, EAGs can provide a qualitative measure of volatile semiochemicals in the atmosphere. Established by Dietrich Schneider (1957) by using the *Bombyx mori* silkworm moth antenna, an EAG response is described as recording the sum of receptor potentials in many sensory neurons by chemical stimuli presented to the antenna (Schneider 1969). The electrical signal from the antenna is collected from electrodes placed at the base and tip of the antenna, amplified, and recorded. EAG response amplitude is dependent on the stimulus concentration and chemical structure. Both EAGs and single-sensillum recordings have been used in tandem with GCMS for determination of biologically relevant volatiles, and EAGs have been used in the field for detection of simulated and natural plumes (Murlis et al. 2000).

Chemical Tracers—Unavailability of fast, sensitive, and affordable chemical detectors for volatile semiochemicals has led to the development of odor plume experiments that rely on surrogate molecules that, optimistically, behave like odor molecules in a plume. Initially, Murlis and Jones (1981) used an ion collector method downwind from an ion generator acting on air at a coastal field to generate a 15 m outdoor plume. Downwind detection of intermittent ion bursts revealed fine scale plume structure, but ion-ion repulsions may have affected plume structure. More recently, gypsy moth pheromone [(+)-disparlure, $C_{19}H_{38}O$] was released synchronously with generated ions upwind and measured by male moth antennae downwind by using EAG. This creative validation approach revealed that pheromone and ion arrival at vertical Langmuir flux probes (ca. 1.2 m^2) was concurrent but quantitatively uncorrelated (Murlis et al. 2000). A more modern surrogate plume approach utilizes fast photoionization detection (PID; up to 330 Hz). Justus et al. (2002, 2005) controlled release of a surrogate propene gas in a 3-m wind tunnel and measured plume structure by using a miniPID from Aurora Scientific (Aurora Scientific Inc., Ontario, Canada). PID continues to offer high temporal resolution of plume structure, but the inherent shortcoming is a lack of discrimination for individual VOCs. Odor concentrations (50–3,000 ppm) measured by PID reflect the sum of all odor mixture components ionized by radiation (8.5–11.7 eV will ionize most organic volatiles $\leq C_{10}$ depending on their respective ionization potentials) from a UV lamp in a detection chamber (Palassis 1997). Development of improved odor stimuli delivery techniques requires high frequency odor detection, which PID can provide (French and Meisner 2007).When coupled with a sonic anemometer, PIDs provide a powerful means to characterize the physical odor environment.

For an insect, the behavioral (odor perception and subsequent navigation) response to an odor is generally immediate (millisecond to minute). The analytical technologies reviewed above and listed in Fig. 4 span a wide range of response times and conceptually fundamental detection methods. As GC is a separation process and not a detection process, GC speed is mainly limited by separation time rather than detection speed. In mass spectrometry, only ions are detected, so the ionization process is fundamental in determining molecule detection efficiency and sample inlet speed. Similar to GC, ion mobility spectroscopy is also a separation process, but ~10^3 times faster than GC (Fig. 4). Laser absorption spectroscopies show promise for trace gas detections in diverse environments, including remote sensing and tomographic applications. The fastest technology reviewed in this paper is photoionization detection (up to 330 Hz; Fig. 4) which Cardé and coworkers have already exploited for several years now (Justus et al. 2002). Other fast techniques shown in Fig. 4 include PTRMS, OPFTIR, LI-COR, EAG, and FIS. Among these, PTRMS, OPFTIR, and EAG have the widest ability to measure diverse chemicals in a single measurement cycle, and may be the most useful techniques going forward in olfactory ecology today.

Summary and Future Directions

The olfactory environment in which insects navigate is dynamic, with physical processes ultimately controlling the chemical signal available to the organism. In this review, we described features of the physical environment that control the dynamics of the chemical signal and a menu of technological innovations that may allow measurement of the fluctuating chemical signal. A multi-disciplinary research approach is thus necessary to effectively investigate and understand the olfactory environment that insects inhabit. Recent advances in analytical technologies allow unprecedented opportunities for chemical ecologists and behavioralists to characterize the physicochemical environment and determine when and where olfactory-mediated behaviors control ecological interactions.

Different physical environments, such as a forest or a desert plain, over land or in water, and the size of an animal body, will affect the chemical stimuli available and may operate as a selective pressure on the sensory system. It follows that different “odor landscapes” will set constraints on insect olfactory systems and odor-tracking navigational behavior. Small insects (<1 mm) inhabit a fluid regime with filamentous odors, but also smooth, sheared odor gradients will exist during periods of limited air movement (Zimmer and Zimmer 2008). In contrast, larger, faster insects inhabit a fluid regime with filamentous and three-dimensional odor. Do insects living at these different scales utilize different behavioral strategies to locate odor sources? Do animals that exist in different environments but inhabit dynamically similar fluid regimes (e.g., a moth and a salmon) use equivalent strategies (see DeBose and Nevitt 2008; Cardé and Willis 2008; Zimmer and Zimmer 2008)? Moreover, much of our understanding of odor plume dynamics comes from sampling at a fixed point. Navigating insects, on the other hand, will be translating in the same space as the filamentous plume and, thus, will be experiencing the plume from a moving reference frame (Lagrangian versus Eulerian frame). How does this influence the chemical signal variation and fine-scale features experienced by the insect? On an evolutionary scale, we might predict that the physicochemical environment has shaped the sensory system and behaviors of these organisms. A comparative, phylogenetic approach presents an exciting opportunity toward an examination of how the physical environment may have influenced organismal sensory systems, behaviors, and morphologies. The improvement of analytical technologies will foster increased understanding of the physicochemical environment and will enable researchers to determine how olfactory environments shape insect behaviors and sensory systems.

Acknowledgments

We thank C. Reisenman, H. Lei, and C. M. Jones for comments during earlier versions of this manuscript. We especially thank H. Thistle, C. A. Zimmer, and R. K. Zimmer for discussions on odor plume dynamics and atmospheric processes. This work was supported by National Institute of Health grant DC-02751 (JGH), National Science Foundation grant CHE-0216226, and a seed grant from the University of Arizona’s Center for Insect Science. J. A. R. was supported by a NIH postdoctoral training grant (2 K12 GM000708-06).

References

Abrell L, Gueresnstein PG, Mechaber WL, Stange G, Christensen TA, Nakanishi K, Hildebrand JG. Effect of elevated atmospheric CO_2 on oviposition behavior in *Manduca sexta* moths. Global Change Biology 2005;11:1272–1282.

Atema J. Eddy chemotaxis and odor landscapes: Exploration of nature with animal sensors. Biol Bull 1996;191:129–138.

Baldocchi DD. Turbulent transfer in a deciduous forest. Tree Physiol 1989;5:357–377. [PubMed: 14972980]

Bargmann CI. Comparative chemosensation from receptors to ecology. Nature 2006;444:295–301. [PubMed: 17108953]

Bau J, Justus KA, Cardé RT. Antennal resolution of pulsed pheromone plumes in three moth species. J Insect Physiol 2002;48:433–442. [PubMed: 12770092]

Bogner F. Sensory physiological investigation of the carbon dioxide receptors in Lepidoptera. J Insect Physiol 1990;36:951–957.

Borsdorf H, Eiceman GA. Ion mobility spectrometry: Principles and applications. Appl Spectrosc Rev 2006;41:323–375.

Cardé RT, Willis MA. Navigation strategies used by insects to find distant, wind-borne sources of odor. J Chem Ecol. 2008this volume

Cermak JE, Arya SPS. Problems of atmospheric shear flows and their laboratory simulation. Boundary-Layer Meteorol 1970;1:40–60.

Charles L, Riter LS, Cooks RG. Direct analysis of semivolatile organic compounds in air by atmospheric pressure chemical ionization mass spectrometry. Anal Chem 2001;73:5061–5065. [PubMed: 11721900]

Chen H, Wortmann A, Zhang W, Zenobi R. Rapid in vivo fingerprinting of nonvolatile compounds in breath by extractive electrospray ionization quadrupole time-of-flight mass spectrometry. Angew Chem Int Ed 2007;46:580–583.

Christian TJ, Kleiss B, Yokelson RJ, Holzinger R, Crutzen PJ, Hao WM, Shitai T, Blake DR. Comprehensive laboratory measurements of biomass-burning emissions: 2. First intercomparison of open-path FTIR, PTR-MS, and GC-MS//FID//ECD J Geophys Res 2004;109:1–12.

Cias P, Wang C, Dibble TS. Absorption cross-sections of the C-H overtone of volatile organic compounds: 2 methyl-1,3-butadiene (isoprene), 1,3-butadiene, and 2,3-dimethyl-1,3-butadiene. Appl Spectrosc 2007;61:230–236. [PubMed: 17331317]

Cody RB, Larame'e JA, Durst HD. Versatile new ion source for the analysis of materials in open air under ambient conditions. Anal Chem 2005;77:2297–2302. [PubMed: 15828760]

Conner WE, Eisner T, Meer RK, Guerrero A, Ghiringelli D, Meinwald J. Sex attractant of an arctiid moth (*Utetheisa ornatrix*): A pulsed chemical signal. Behav Ecol Sociobiol 1980;7:55–63.

Cooks RG, Ouyang Z, Takats Z, Wiseman JM. Ambient mass spectrometry. Science 2006;311:1566–1570. [PubMed: 16543450]

D'Alessandro M, Turlings TCJ. Advances and challenges in the identification of volatiles that mediate interactions among plants and arthropods. Analyst 2006;131:24–32. [PubMed: 16365659]

De gouw J, Warneke C. Measurements of volatile organic compounds in the Earth's atmosphere using proton-transfer-reaction mass spectrometry. Mass Spectrom Rev 2007;26:223–257. [PubMed: 17154155]

Debose JL, Nevitt GA. Behavioral responses and navigational strategies to natural olfactory stimuli II: fish and birds. J Chem Ecol. 2008this volume

Dinar N, Kaplan H, Kleiman M. Characterization of concentration fluctuations of a surface plume in a neutral boundary layer. Boundary-Layer Metereol 1988;45:157–175.

Dorfner R, Ferge T, Yeretzian C, Kettrup A, Zimmermann R. Laser mass spectrometry as on-line sensor for industrial process analysis: Process control of coffee roasting. Anal Chem 2004;76:1386–1402. [PubMed: 14987096]

Eiceman GA, Snyder AP, Blyth DA. Monitoring of airborne organic vapors using ion mobility spectrometry. I J Env Anal Chem 1990;38:415–425.

Elkinton JS, Cardé RT, Mason CJ. Evaluation of time-average dispersion models for estimating pheromone concentration in a deciduous forest. J Chem Ecol 1984;10:1081–1108.

Fackrell JE, Robins AG. The effects of source size on concentration fluctuations in plumes. Boundary-Layer Meteorol 1982;22:335–350.

Filella I, Penuelas J, Llusia J. Dynamics of the enhanced emissions of monoterpenes and methyl salicylate, and decreased uptake of formaldehyde, by *Quercus ilex* leaves after application of jasmonic acid. New Phytologist 2006;169:135–144. [PubMed: 16390425]

Finelli CM, Pentcheff ND, Zimmer-Faust RK, Wethey DS. Odor Transport in Turbulent Flows: Constraints on Animal Navigation. Limnol Oceanogr 1999;44:1056–1071.

Finelli CM, Pentcheff N, Zimmer RK, Wethey DS. Physical constraints on ecological processes: A field test of odor-mediated foraging. Ecology 2000;81:784–797.

Freeman CG, Mcewan MJ. Rapid analysis of trace gases in complex mixtures using selected ion flow tube-mass spectrometry. Australian J Chem 2002;55:491–494.

French AS, Meisner S. A new method for wide frequency range dynamic olfactory stimulation and characterization. Chem Senses 2007;32:681–688. [PubMed: 17566069]

Guerenstein P, Guerin P. Olfactory and behavioural responses of the blood-sucking bug *Triatoma infestans* to odours of vertebrate hosts. J Exp Biol 2001;204:585–597. [PubMed: 11171309]

Guerenstein P, Christensen TA, Hildebrand JG. Sensory processing of ambient CO_2 information in the brain of the moth *Manduca sexta*. J Comp Physiol A 2004;190:707–725.

Guerenstein P, Hildebrand JG. Roles and effects of environmental carbon dioxide in insect life. Annu Rev Entomol 2008;53:161–178. [PubMed: 17803457]

Haefliger OP, Jeckelmann N. Direct mass spectrometric analysis of flavors and fragrances in real applications using DART. Rapid Commun Mass Spectrom 2007;21:1361–1366. [PubMed: 17348088]

Heinbockel T, Christensen TA, Hildebrand JG. Temporal tuning of odor responses in pheromone-responsive projection neurons in the brain of the sphinx moth *Manduca sexta*. J Comp Neurol 1999;409:1–12. [PubMed: 10363707]

Hildebrand JG. Analysis of chemical signals by nervous systems. Proc Natl Acad Sci USA 1995;92:67–74. [PubMed: 7816849]

Hills AJ, Zimmerman PR. Isoprene measurement by ozone-induced chemiluminescence. Anal Chem 1990;62:1055–1060.

Ho CK, Robinson A, Miller DR, Davis MJ. Overview of sensors and needs for environmental monitoring. Sensors 2007;5:4–37.

Iwana T, Mitsutaka H, Isao Y, Okada H, Hiraoka K. Development of sniffing atmospheric pressure Penning ionization. J Mass Spectrom Soc Japan 2006;54:227–233.

Jublot L, Linforth RST, Taylor AJ. Direct atmospheric pressure chemical ionisation ion trap mass spectrometry for aroma analysis: Speed, sensitivity and resolution of isobaric compounds. I J Mass Spectrom 2005;243:269–277.

Justus KA, Murlis J, Jones CD, Cardé RT. Measurement of odor-plume structure in a wind tunnel using photoionization detector and a tracer gas. Env Fluid Mech 2002;2:115–142.

Justus KA, Cardé RT, French AS. Dynamic properties of antennal responses to pheromone in two moth species. J Neurophysiol 2005;93:2233–2239. [PubMed: 15537812]

Kachanov AA, Crosson ER, Paldus BA. Tunable diode lasers: Expanding the horizon for laser absorption spectroscopy. Optics Photonics News 2006;16:44–50.

Kaimal, J.; Finnigan, J. Atmospheric Boundary Layer Flows. Vol. 1. Oxford University Press; Oxford: 1994.

Kaissling KE, Priesner E. Die Riechschwelle des Seidenspinners. Naturwissenschaften 1970;57:23–28. [PubMed: 5417282]

Karl T, Guenther A, Jordan A, Fall R, Lindinger W. Eddy covariance measurement of biogenic oxygenated VOC emissions from harvesting. Atmos Env 2000;35:491–495.

Karl T, Jobson T, Kuster WC, Williams E, Stutz J, Shetter R, Hall SR, Goldan P, Fehsenfeld F, Lindinger W. Use of proton-transfer-reaction mass spectrometry to characterize volatile organic compound sources at the La Porte super site during the Texas Air Quality Study 2000. J Geophys Res 2003;108:ACH13–1–ACH13/15.

Khunemann F, Wolfertz M, Arnold S, Lagemann M, Popp A, Schuler U, Jux A, Boland W. Simultaneous online detection of isoprene and isoprene-d_2 using infrared photoacoustic spectroscopy. App Physics B 2002;75:397–403.

Kleineidam C, Roces F. Carbon dioxide concentrations and nest ventilation in nests of the leaf-cutting ant *Atta vollenweideri*. Insectes Sociaux 2000;47:241–248.

Kleineidam C, Ernst R, Roces F. Wind-induced ventilation of the giant nests of the leaf-cutting ant *Atta vollenweideri*. Naturwissenschaften 2001;88:301–305. [PubMed: 11544898]

Koehl MAR. The fluid mechanics of arthropod sniffing in turbulent odor plumes. Chem Senses 2006;31:93–105. [PubMed: 16339271]

Kuenen L, Carde RT. Strategies for recontacting a lost pheromone plume: Casting and upwind flight in the male gypsy moth. Physiol Entomol 1994;19:15–29.

Kunert M, Biedermann A, Koch T, Boland W. Ultrafast sampling and analysis of plant volatiles by a hand-held miniaturised GC with pre-concentration unit: Kinetic and quantitative aspects of plant volatile production. J Sep Sci 2002;25:677–684.

Lambertus GR, Fix CS, Reidy SM, Miller RA, Wheeler D, Nazarov E, Sacks R. Silicon microfabricated column with microfabricated differential mobility spectrometer for GC analysis of volatile organic compounds. Anal Chem 2005;77:7563–7571. [PubMed: 16316163]

Leclerc MY, Meskhidze N, Finn D. Comparison between measured tracer fluxes and footprint model predictions over a homogeneous canopy of intermediate roughness. Agric For Meteorol 2003;117:145–158.

Lindinger W, Hansel A, Jordan A. Proton-transfer-reaction mass spectrometry (PTR-MS): on-line monitoring of volatile organic compounds at pptv levels. Chem Soc Rev 1998a;27:347–354.

Lindinger W, Hansel A, Jordan A. On-line monitoring of volatile organic compounds at pptv levels by means of proton-transfer-reaction mass spectrometry (PTR-MS). Medical applications, food control, and environmental research. I J Mass Spectrom 1998b;173:191–241.

Lu CJ, Zellers ET. Multi-adsorbent preconcentration/focusing module for portable-GC/microsensor-array analysis of complex vapor mixtures. Analyst 2002;127:1061–1068. [PubMed: 12195947]

Mafra-Neto A, Carde RT. Fine-scale structure of pheromone plumes modulates upwind orientation of flying moths. Nature 1994;369:142–144.

Matisola E, Dömötörová M. Fast gas chromatography and its use in trace analysis. J Chromatogr A 2003;1000:199–221. [PubMed: 12877172]

Miller JR, Roelofs WL. Sustained-flight tunnel for measuring insect responses to wind-borne sex pheromones. J Chem Ecol 1978;4:187–198.

Mole N, Jones CD. Concentration fluctuation data from dispersion experiments carried out in stable and unstable conditions. Boundary-Layer Meteorol 1994;67:41–74.

Moore PA, Atema J. Spatial information in the three-dimensional fine structure of an aquatic odor plume. Biol Bull 1991;181:408–418.

Moore P, Crimaldi J. Odor landscapes and animal behavior: tracking odor plumes in different physical worlds. J Mar Sys 2004;49:55–64.

Murlis, J. Odor plumes and the signal they provide. In: Carde, RT.; Minks, AK., editors. Insect Pheromone Research: New Directions. Chapman and Hall; New York: 1997. p. 221-231.

Murlis J, Jones C. Fine-scale structure of odour plumes in relation to insect orientation to distant pheromone and other attractant sources. Physiol Entomol 1981;6:71–86.

Murlis J, Elkinton JS, Carde RT. Odor plumes and how insects use them. Annu Rev Entomol 1992;37:505–532.

Murlis J, Willis MA, Carde RT. Spatial and temporal structures of pheromone plumes in fields and forests. Physiol Entomol 2000;25:211–222.

Mustaparta H. Responses of single olfactory cells in the pine weevil *Hylobius abietis* L. (Col: Curculionidae). J Comp Physiol A 1975;97:271–290.

Mylne KR. Concentration fluctuation measurements in a plume dispersing in a stable surface layer. Boundary-Layer Meteorol 1992;60:15–48.

Mylne KR, Davidson MJ, Thomson DJ. Concentration fluctuation measurements in tracer plumes using high and low frequency response detectors. Boundary-Layer Meteorol 1996;79:225–242.

Mylne K, Mason P. Concentration fluctuation measurements in a dispersing plume up to a range of 1000 m. Quart J Roy Meteorol Soc 1991;117:177–206.

Ngai AKY, Persijn ST, Harren FJM, Verbraak H, Linnartz H. Selective trace gas detection of complex molecules with a continuous wave optical parametric oscillator using a planar jet expansion. Appl Phys Lett 2007;90:081109–1–081109–3.

Palassis J. Portable photoionization instruments. Appl Occup Environ Hyg 1997;12:528–531.

Park KC, Ochieng SA, Zhu J, Baker TC. Odor discrimination using insect electroantennogram responses from an insect antennal array. Chem Senses 2002;27:343–352. [PubMed: 12006374]

Rauner, JL. Deciduous forests. In: Monteith, JL., editor. Vegation and the Atmosphere, Vol. II Case Studies. Academic Press; London: 1976. p. 241-264.

Reidy S, George D, Agah M, Sacks R. Temperature-programmed GC using silicon microfabricated columns with integrated heaters and temperature sensors. Anal Chem 2007;79:2911–2917. [PubMed: 17311465]

Röck F, Barsan N, Weimar U. Electronic nose: Current status and future trends. Chem Rev 2008;108:705–725. [PubMed: 18205411]

Roelofs, WL. Electroantennogram assays: Rapid and convenient screening procedures for pheromones. In: Hummel, HE.; Miller, TA., editors. Techniques in Pheromone Research. Springer; New York: 1984. p. 131-159.

Sanchez JM, Sacks R. Performance characteristics of a new prototype for a portable GC using ambient air as carrier gas for on-site analysis. J Sep Sci 2007;30:1052–1060. [PubMed: 17566340]

Schlichting, H. Boundary-Layer Theory. Vol. 8. McGraw-Hill; New York: 1987.

Schneider D. Elektrophysiologishe untersuchungen von chemo-und mechanorezeptoren der antennne des Seidenspinners *Bombyx mori* L. *Z Vergi*. Physiol 1957;40:8–41.

Schneider D. Insect olfaction: Deciphering system for chemical messages. Science 1969;163:1031–1037. [PubMed: 4885069]

Song MS, Marriotr P, Ryant D, Wynne P. Analytical limbo: How low can you go? LCGC North America 2006;24:1012–1029.

Sprayberry JDH, Daniel TL. Flower tracking in hawkmoths: behavior and energetics. J Exp Biol 2007;210:37–45. [PubMed: 17170146]

Stange, G. Sensory and behavioural responses of terrestrial invertebrates to biogenic carbon dioxide gradients. In: Stanhill, G., editor. Advances in Bioclimatology. Springer; Heidelberg: 1996. p. 223-253.

Stange G. Effects of changes in atmospheric carbon dioxide on the location of hosts by the moth, *Cactoblastis cactorum*. Oecologia 1997;110:539–545.

Stull, RB. An Introduction to Boundary Layer Meteorology. Kluwer; Dordrecht: 1988.

Stranden M, Liblikas I, König WA, Almaas TJ, Borg-Karlson AK, Mustaparta H. (−)-Germacrene D receptor neurones in three species of heliothine moths: structure-activity relationships. J Comp Physiol A 2003;189:563–577.

Thistle HH, Peterson H, Allwine G, Lamb B, Strand T, Holsten EH, Shea PJ. Surrogate Pheromone plumes in three forest trunk spaces: composite statistics and case studies. For Sci 2004;50:610–625.

Tholl D, Boland W, Hansel A, Loreto F, Röse USR, Schnitzler JP. Practical approaches to plant volatile analysis. Plant J 2006a;45:540–560. [PubMed: 16441348]

Tholl, D.; Röse, USR. Detection and identification of floral scent compounds. In: Dudavera, N.; Pichersky, E., editors. Biology of Floral Scent. CRC; Boca Raton, FL: 2006b. p. 3-25.

Todd L. Mapping the air in real-time to visualize the flow of gases and vapors: occupational and environmental applications. Appl Occup Environ Hyg 2000;15:106–113. [PubMed: 10660996]

Vickers NJ, Baker TC. Reiterative responses to single strands of odor promote sustained upwind flight and odor source location by moths. Proc Natl Acad Sci USA 1994;91:5756–5760. [PubMed: 11607476]

Vickers NJ, Baker TC. Latencies of behavioral response to interception of filaments of sex pheromone and clean air influence flight track shape in *Heliothis virescens* (F.) males. J Comp Physiol A 1996;178:831–847.

Visser JH. The design of a low-speed wind tunnel as an instrument for the study of olfactory orientation in the Colorado beetle (*Leptinotarsa decemlineata*). Ent Exp Appl 1976;20:275–288.

Vogt F. Trends in remote spectroscopic sensing and imaging -experimental techniques and chemometric concepts. Cur Anal Chem 2006;2:107–127.

Von dahl CC, Heavecker M, Schloegl R, Baldwin IT. Caterpillar-elicited methanol emission: A new signal in plant-herbivore interactions? Plant J 2006;46:948–960. [PubMed: 16805729]

Wang C, Mbi A. A new acetone detection device using cavity ringdown spectroscopy at 266 nm: evaluation of the instrument performance using acetone sample solutions. Meas Sci Tech 2007;18:2731–2741.

Webster DR, Weissburg MJ. Chemosensory guidance cues in a turbulent chemical odor plume. Limnol Oceanogr 2001;46:1034–1047.

Weissburg MJ. The fluid dynamical context of chemo-sensory behavior. Biol Bull 2000;198:188–202. [PubMed: 10786940]

Weissburg MJ, Zimmer-Faust RK. Life and death in moving fluids: Hydrodynamic effects on chemosensory-mediated predation. Ecology 1993;74:1428–1443.

Whalley LK, Lewis AC, Mcquaid JB, Purvis RM, Lee JD, Stemmler K, Zellweger C, Ridgeopn P. Two high-speed, portable GC systems designed for the measurement of non-methane hydrocarbons and PAN: Results from the Jungfraujoch high altitude observatory. J Env Mon 2004;6:234–241.

Willis MA, David CT, Murlis J, Cardé RT. Effects of pheromone plume structure and visual stimuli on the pheromone-modulated upwind flight of male gypsy moths (*Lymantria dispar*) in a Forest (Lepidoptera: Lymantriidae). J Insect Behav 1994;7:385–409.

Willis MA, Baker TC. Effects of varying sex pheromone component ratios on the zigzagging flight movements of the oriental fruit moth, *Grapholita molesta*. J Insect Behav 1988;1:357–371.

Wolf H, Wehner R. Pinpointing food sources: olfactory and anemotactic orientation in desert ants, *Cataglyphis fortis*. J Exp Biol 2000;203:857–868. [PubMed: 10667968]

Yee E, Kosteniuk PR, Chandler GM, Biltoft CA, Bowers JF. Statistical characteristics of concentration fluctuations in dispersing plumes in the atmospheric surface layer. Boundary-Layer Meteorol 1993;65:69–109.

Zimmer RK, Butman CA. Chemical signaling processes in the marine environment. Biol Bull 2000;198:168–187. [PubMed: 10786939]

Zimmer RK, Zimmer CA. Dynamic scaling in chemical ecology. J Chem Ecol. 2008this volume

Zimmer-Faust RK, Stanfill JM, Collard SB. A fast, multi-channel fluorometer for investigating aquatic chemo-reception and odor trails. Limnol Oceanogr 1988;33:1586–1594.

Zimmer-Faust RK, Finelli CM, Pentcheff ND, Wethey DS. Odor plumes and animal navigation in turbulent water flow: A field study. Biol Bull 1995;188:111–116.

Zimmermann R. Laser ionisation mass spectrometry for online analysis of complex gas mixtures and combustion effluents. Anal Bioanal Chem 2005;381:57–60. [PubMed: 15619086]

Zollner GE, Torr SJ, Ammann C, Meixner FX. Dispersion of carbon dioxide plumes in African woodland: implications for host-finding by tsetse flies. Physiol Entomol 2004;29:381–394.

Appendix 1

Table 1

Notation for physical processes

Symbol	Definition	Units
D	Roughness element height (Eq. 3)	m
D_{object}	Diameter of object used in Strouhal number calculation (Eq. 5)	m
f	Eddy shedding frequency (Eq. 5)	1/s
G	Gravitational acceleration.	m/s^2
μ	Air viscosity (Eq. 1)	Ns/m^2
p	Air density (Eq. 1)	kg/m^3
N	Frequency of the peak intensity of velocity spectra	1/s
Re	Reynolds number (Eq. 1). The ratio between inertial and viscous forces, $Re = \frac{\rho S u}{\mu}$	dimensionless
Re_*	Reynolds roughness number (Eq. 3). Describes boundary layer, $Re_{\square} = \frac{\rho u_{\square} D}{\mu}$	Dimensionless
R_i	Richardson number (Eq. 4). Describes boundary layer stability, $R_i = \frac{(g/\theta)(\partial\theta/\partial z)}{(\partial\bar{u}/\partial z)^2}$	Dimensionless
S	Insect spatial scale (Eq. 1)	M
S_t	Strouhal number (Eq. 5). Eddy shedding frequency by objects in wind. $St = \frac{f D_{object}}{u}$	Dimensionless
u	Velocity in the horizontal dimension (Eq. 1)	m/s

Symbol	Definition	Units
$\bar{u}$	Mean horizontal velocity (Eq. 1)	m/s
u'	Fluctuating horizontal velocity (Eq. 2)	m/s
u_*	Friction velocity (Eq. 3). Describes intensity of the turbulence	m/s
w	Velocity in the vertical dimension (Eq. 2)	m/s
w'	Fluctuating vertical velocity (Eq. 2)	m/s
τ_R	Reynolds shear stress (Eq. 2), $\tau_R = -\rho\overline{u'w'}$.	N/m^2
z	Height above the substrate (Eq. 4)	m
$\bar{\theta}$	Mean temperature (Eq. 4)	Kelvin

Appendix 2

Table 2

Notation for analytical technologies

Category	Technique abbreviation	Technique
Gas chromatography	GCMS	Gas chromatography mass spectrometry
	GCSAW	Gas chromatography surface acoustic wave quartz microbalance detection
	GCHID	Gas chromatography helium ionization detection
	GCECD	Gas chromatography electron capture detection
Chemical ionization mass spectrometry	PTRMS	Proton transfer reaction mass spectrometry
	SIFTMS	Selected ion flow tube mass spectrometry
	LCITMS	Liquid chromatography ion trap mass spectrometry
	DESIMS	Desorption electrospray ionization mass spectrometry
	DARTMS	Direct analysis in real time mass spectrometry
	APPeITOFMS	Atmospheric pressure Penning ionization time of flight mass spectrometry
	REMPIMS	Resonance-enhanced multiphoton ionization mass spectrometry
	SPIMS	Single photon ionization mass spectrometry
	EESIMS	Extractive electrospray ionization mass spectrometry
Ion mobility spectroscopy	IMS	Ion mobility spectroscopy
	GCDMS	Gas chromatography differential mobility spectroscopy
	GCFAIMS	Gas chromatography high-field asymmetric waveform ion mobility spectrometry
Absorption spectroscopy	OPFTIR	Open-path Fourier transform infrared spectroscopy
	CRDS	Cavity ringdown spectroscopy
	TDLAS	Tunable diode laser absorption spectroscopy
	PAS	Photo acoustic spectroscopy
	IRGA	Infrared gas analyzer
	LICOR	Refers to the LI-7500 non-dispersive infrared CO_2/H_2O gas analyzer from LI-COR Biosciences
Chemiluminescence	FIS	Fluorescent isoprene sensor
Other	EAG	Electroantennography
	PID	Photoionization detection

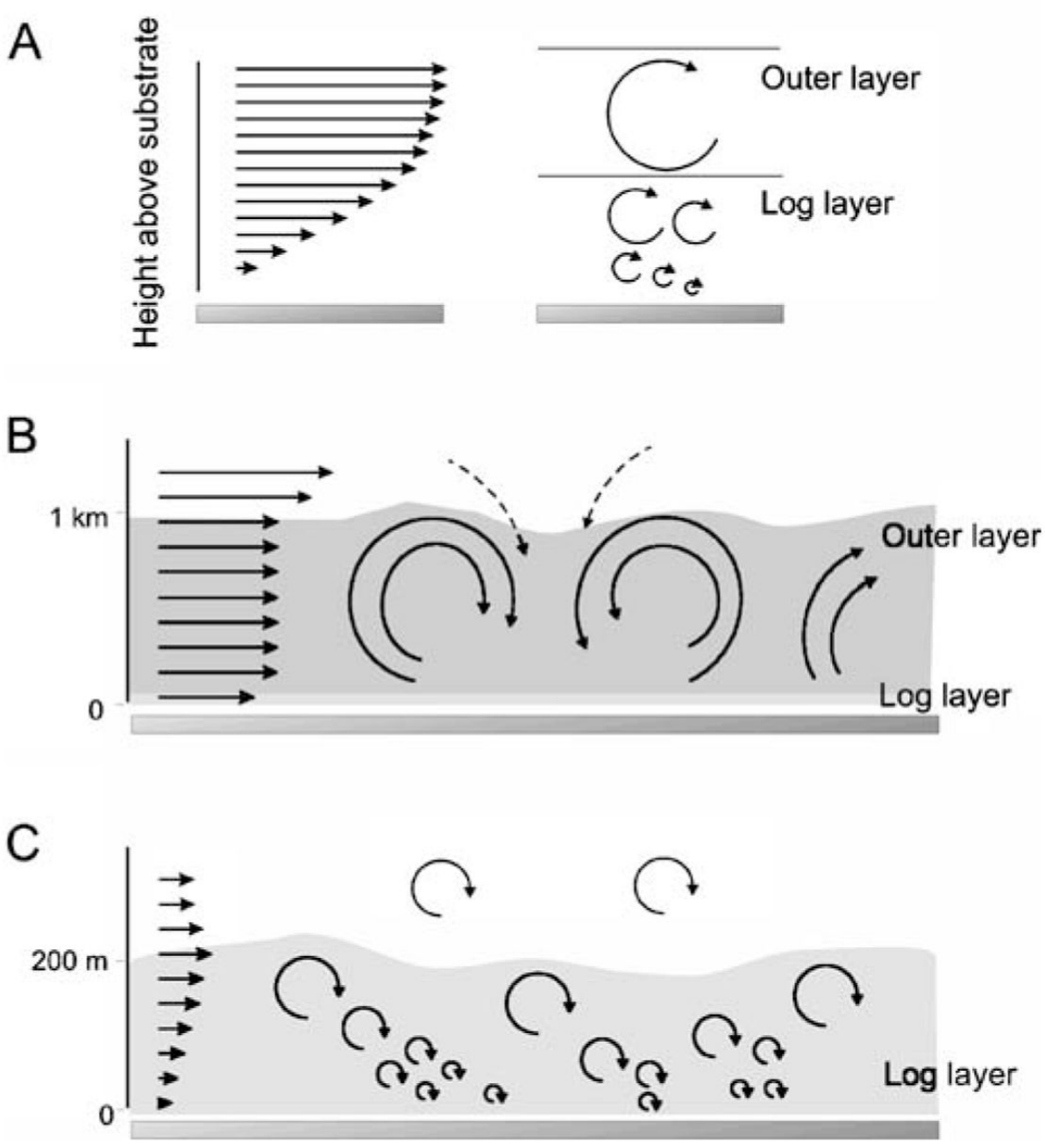

Fig. 1.

The effect of flow velocity on the structure within a turbulent boundary layer and the change in diurnal conditions. **A** The boundary layer is defined by the region where the flow velocity reaches 95% of the free stream velocity (*left*). A schematic of the turbulent velocity fluctuations is shown on the right where turbulent kinetic energy is transferred from the large energy-containing eddies in the outer region of the boundary layer to progressively smaller and smaller eddies in the log layer. **B** A schematic of the daytime boundary layer conditions where surface-layer heating causes the large eddies in the outer layer to reach all the way to the substratum. **C** A schematic of the nighttime boundary layer conditions. Substrate cooling causes a stable

boundary layer to develop and the kinetic turbulent energy levels to drop in comparison to daytime turbulent conditions

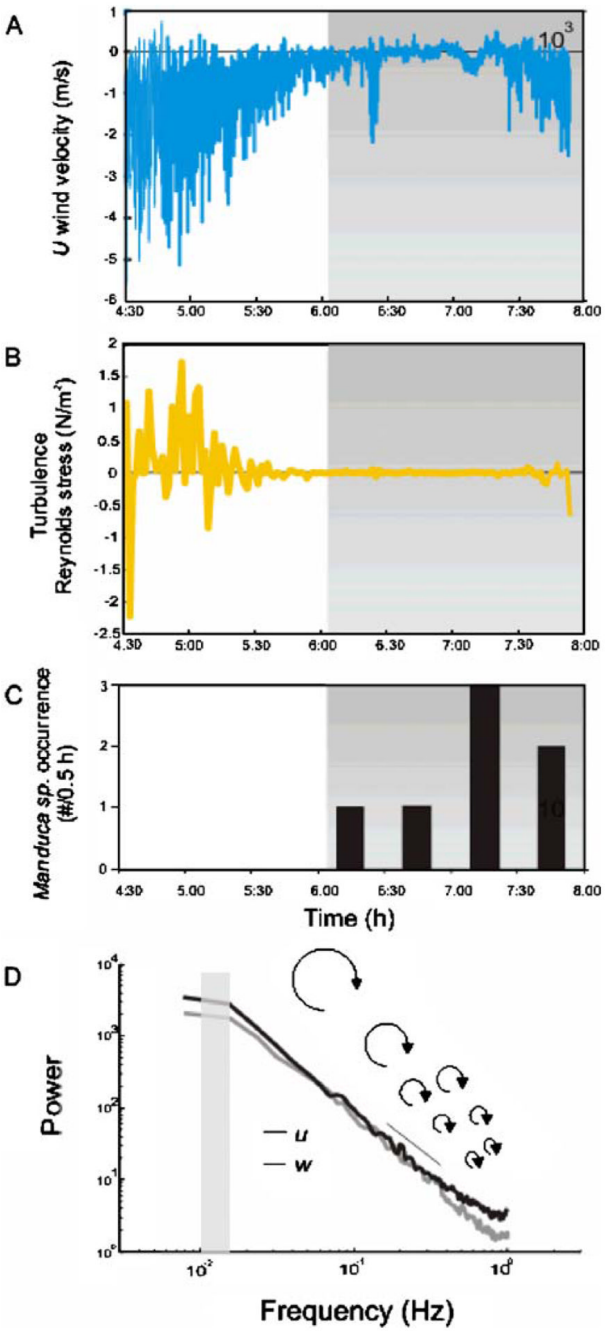

Fig. 2.

A time series of the turbulent conditions near a *Datura wrightii* flower patch measured with a 3D sonic anemometer (Young, USA) sampling at 32 Hz. Regions in gray represent the time from when the sun began to set. In the daytime, wind velocities (**A**) and turbulent shear stresses (**B**) are nearly two-orders of magnitude higher then those that occur in the evening (shown in *gray*). **C** The drop in turbulent intensities corresponds with the nighttime foraging activity by *Manduca sexta* hawkmoths which feed on nectar from *D. wrightii* flowers. The drop in turbulent intensities may enable hawkmoths to effectively navigate to the strong volatile emissions of *D. wrightii* flowers. **D** Daytime energy spectra of wind velocities in the vertical (*w*) and longitudinal (*u*) dimensions. The largest energy-bearing eddies (in *shaded region*)

occur at a time period of 100 s (frequencies ~10^{-2} Hz), and corresponds to *n*, where *n* is the frequency of peak intensity of the power spectrum. The large eddies progressively cascade smaller and smaller eddies until the turbulent kinetic energy is dissipated at a frequency of 0.8 Hz. Spectra of the velocity fluctuations contain information on the temporal and spatial features of the turbulence and relate directly to dispersion and structure of the plume

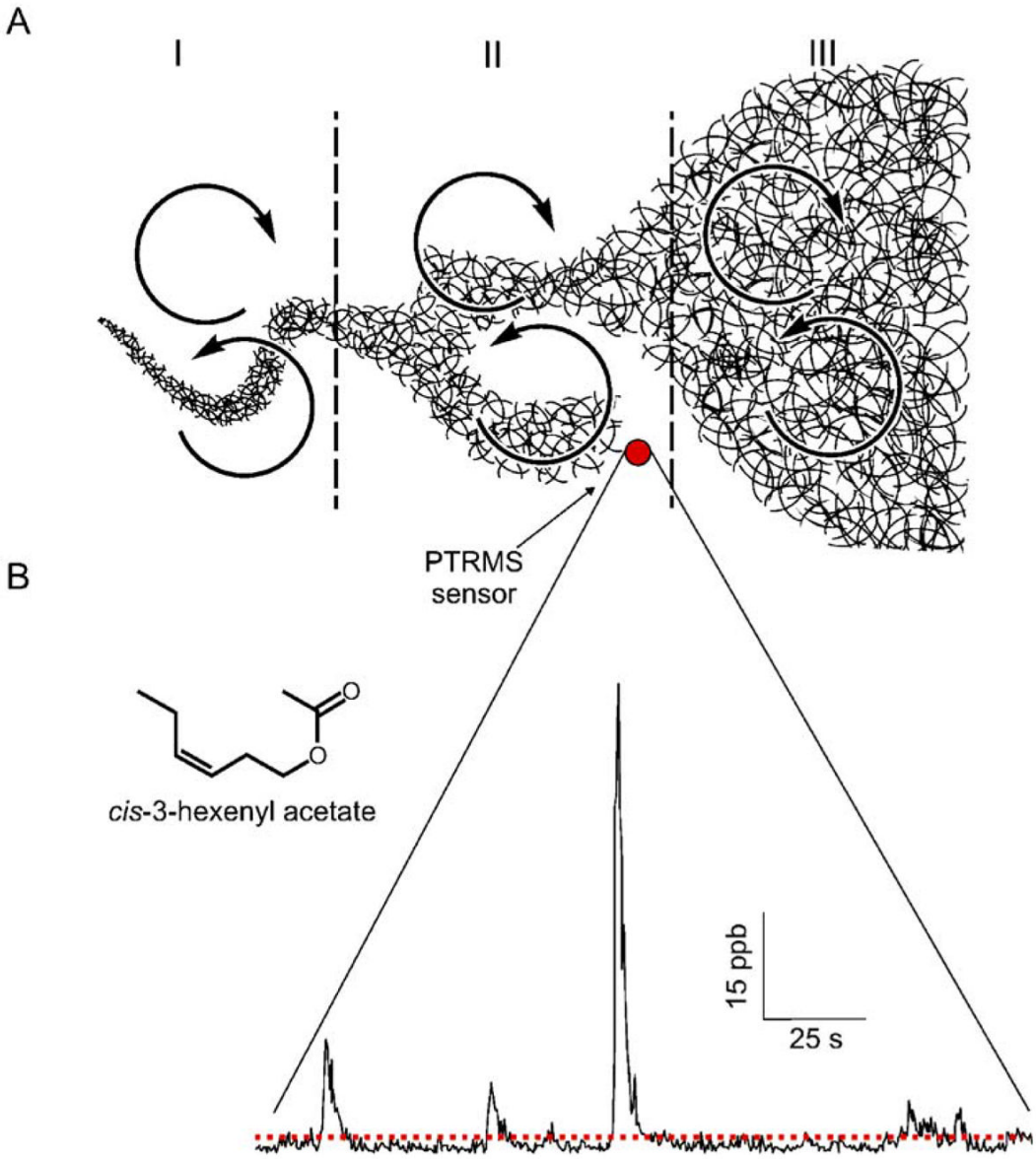

Fig. 3.

Odor plumes are spatio-temporally dynamic. **A** A schematic of a conceptual model for plume dispersion modified from Mylne (1992). When the plume width is smaller than the dominant crosswind eddy size the plume will begin meandering. Once the plume width approaches the eddy size the plume becomes mixed with clean air. The plume will continue to develop and increase in size until its width exceeds the eddy scale (Environmental Effects on the Odor Landscape). The plume structure as a whole will depend upon the dominant eddy scale and the variation in concentration fluctuations of the plume. **B** A mass chromatogram of a *cis*-3-hexenyl acetate ($C_8H_{14}O_2$) plume as measured by proton transfer reaction mass spectrometry (*PTRMS*). Measurements occurred 4 m downwind from the source at an average wind velocity of 40 cm/s, dominant eddy size of 2.1 m and frequencies of 10 s. Based on conditional sampling of the plume measurements, odor bursts occurred every 11.1 s which approximately matched those predicted by Mylne (1992). The PTRMS sample rate was 4 Hz

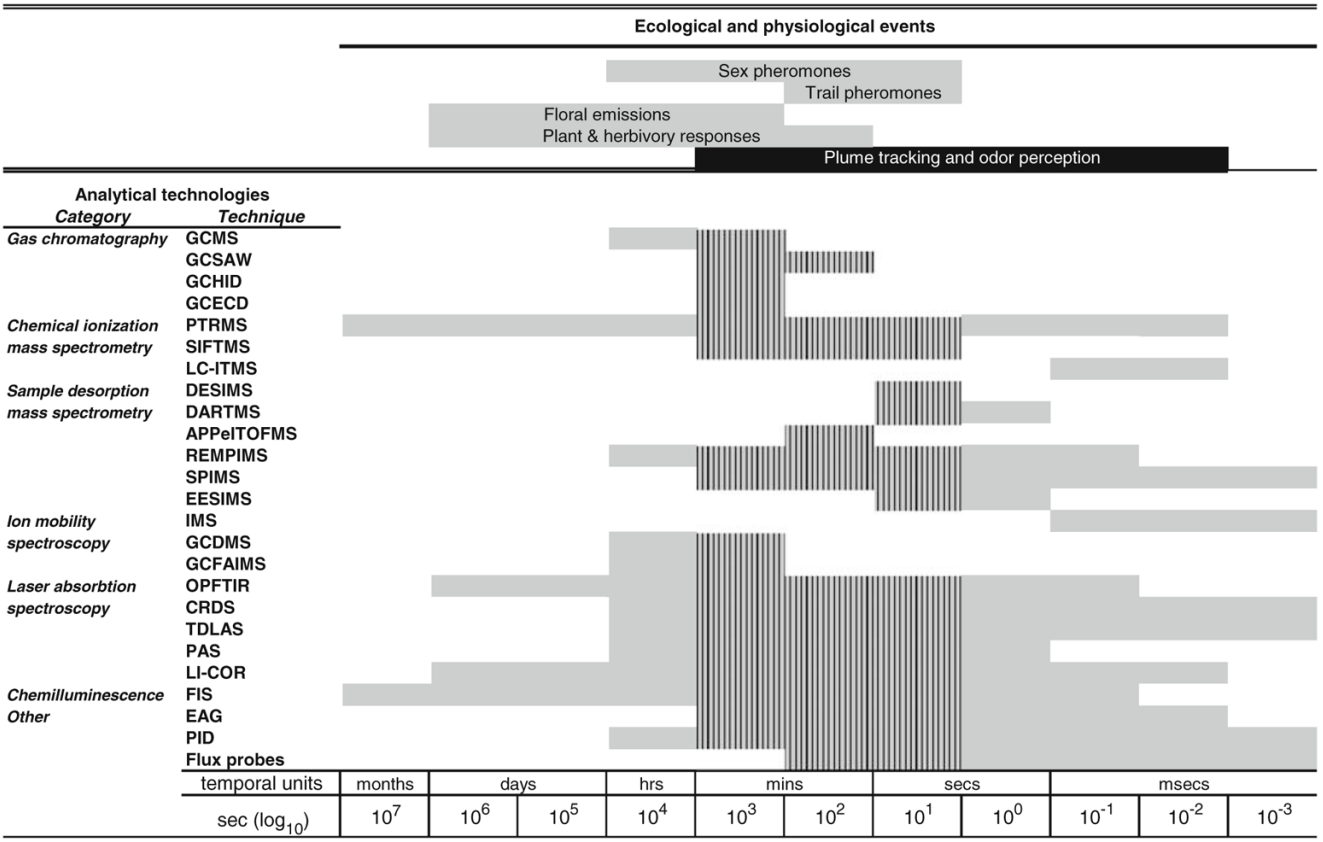

Fig. 4.

Ecological and odor producing physiological activities (*upper five rows*) are compared with available analytical technologies having potential application in olfactory ecology. Ecological events are portrayed as two types: odor emissions (*gray*) lasting from seconds to hours, and odor tracking and perception (*black*) lasting from milliseconds to minutes. Temporal resolution ranges (in seconds; *lower rows*; log scale) obtainable from measurements with analytical technologies listed by category (acronyms defined in "Analytical Equipment", see also Appendix 2) are shown in *gray*. The temporal range where chemical signal emission and signal reception (olfaction) overlap is indicated by *hashed marks*